Antarctic non-stationary signals derived from Seasat–ERS-1 altimetry comparison

FRÉDÉRIQUE RÉMY, BENOÎT LEGRÉSY

UMR5566/GRGS (CNES–CNRS–UPS), 18 av. E. Belin, 31401 Toulouse Cedex 4, France

ABSTRACT. Geographical changes in the height of the Antarctic ice sheet between 1978 and 1992 are mapped using altimeter data from Seasat and ERS-1 via an inverse technique that allows us to take into account the whole altimetric error budget. In a belt between 70° and 72° S and between 150° and 80° E, a precision better than 40 cm is found for the surface elevation change, while the change in height averaged in the along-slope direction has a precision of around 10–20 cm, leading to a precision better than 10% of the mass balance. These data suggest a relative positive imbalance of around 20% in this sector for the western and high-altitude areas, and a relative negative imbalance in some areas of lower altitude.

1. INTRODUCTION

The launch of Seasat nearly 20 years ago, followed by that of Geosat 6 years later, provided the first altimetric measurements over continental ice sheets, south of 72° N for Greenland and north of 72° S for Antarctica. These observations quickly assumed considerable importance both for ice-sheet modeling studies, by providing precise surface topography (Young and others, 1989; Rémy and Minster, 1997), and for ice-sheet surface-state studies (Rémy and others, 1990). Zwally and others (1989) demonstrated the potential of a long-term survey of Greenland with the twin Seasat and Geosat satellites. Since 1991 the precision and coverage of the ERS-1 radar altimeter has helped provide a very accurate surface topography covering 80% of the Antarctic ice sheet, which may now contribute significantly to glaciological studies at both synoptic and long-term scales. ERS-2, launched in 1995, and ENVISAT, planned to be launched in mid-1999, have the same orbit characteristics (altitude, inclination, repetitivity), as well as the same antenna characteristics (Ku-band radar wavelength, antenna diameter), in order to optimize the long-term survey of ice-sheet topography.

In the meantime, Seasat altimeter data exist and should be compared with ERS data. Differences between the two satellite missions require some specific errors to be taken into account: (1) the difference in sampling between Seasat and ERS-1 allows only a discrete comparison at crossover points; (2) the difference between the altitudes of the two satellites induces difference in slope error; (3) the difference between antenna characteristics causes a difference in volume-induced error (Legrésy and Rémy, 1997); and (4) the differences between Seasat and ERS data processing, at both instrumental and geophysical levels, require a reprocessing of the entire datasets, particularly with regard to atmospheric or retracking corrections.

To compare the two datasets, we use a total inverse technique that allows the data to be analyzed by taking into account any statistical knowledge of their errors. In section 2 of this paper, we describe the data processing and explain the statistical characteristics of all errors. In section 3 we suggest possible interpretations of change in height.

2. MAPPING OF THE DIFFERENCE BETWEEN SEASAT AND ERS-1 HEIGHTS

2.1. Data processing

The basic Seasat dataset is composed of waveform data from the Seasat SDR (sensor data record) from September to October 1978. ERS-1 waveform altimeter product (WAP) from the 35 day orbit phase delivered by the U.K. Processing and Archiving Facility is used. In order to ensure a maximum ERS coverage, we selected five ERS-1 35 day repeat cycles. The selected cycles (Nos. 83, 85, 87, 89, 97) from 14 April 1992 to 3 September 1993 are chosen with the altimeter working in ocean mode, to ensure a waveform resolution comparable to that for Seasat. Cycle 87 (14 August–18 September) is taken as the reference set to minimize potential seasonal effects.

Both datasets are reprocessed with the same algorithms, especially in terms of the retracking technique which consists of fitting each waveform to an error function (Féménias and others, 1993). Comparison between both backscattering coefficients is also needed to correct for apparent change in height induced by change in snow-surface characteristics (Ridley and Bamber, 1995; Legrésy and Rémy, in press). Thus, in the same way, both backscattering coefficients are corrected for the shift of the waveform inside the received window (Rémy and others, 1990) within the retracking algorithm. NASA Goddard Space Flight Center orbits are used for Seasat, and precise orbits from Delft University for ERS-1. In both cases, the heights are given with respect to the World Geodetic System 1984 ellipsoid.

It is noticeable that the estimated error after mapping the topography from altimetric data from a given satellite shows a strong correlation with the geographical sampling

(Rémy and others, 1989; Brisset and Rémy, 1996) because of the 10 km scale topographic signal that is due to the presence of undulations. The direct comparison of two independent maps derived from different satellite missions with different geographical samplings would then be controlled by this important short-scale signal. We consider here the difference in height at the Seasat–ERS crossover locations (Fig. 1a). We have about 1800 crossover points between Seasat data and each ERS-1 cycle, leading to a total of 9000 crossover points.

2.2. Statistical description of error term

In order to reduce the remaining error after reprocessing, we used a total inverse technique adapted to ice-sheet mapping (Rémy and others, 1989). Each term of the error budget is taken into account by describing its statistics in terms of a covariance function and a decorrelation length. Knowledge of the statistics of the various components of the residual error helps separate the error from the signal. If $\delta^{i,j}$ is the difference between two quantities from track i of Seasat and track j of ERS, and if d is the signal we are looking for and h is the observed height difference, one can write:

$$\delta^{i,j}h(x,y) = \delta^{i,j}d(x,y) + \delta^{i,j}e_1 + \delta^{i,j}e_{\text{atm}}$$
$$+ \delta^{i,j}e_{\text{orb}} + \delta^{i,j}e_{\text{slope}} + \delta^{i,j}e_{\text{ret}} + \delta^{i,j}e_{\text{snow}} \quad (1)$$

where e_1 is the instrument noise, including retracking noise, assumed to be white with a 30 cm rms amplitude. The associated covariance is a Dirac-delta function for each instrument. e_{tm} is the error due to atmospheric and ionospheric errors. The dominant tropospheric error, the dry atmospheric error, is not corrected for since it depends on the local ice-sheet height of the measurement and is the same for both missions. Because of the spatio-temporal sampling, two different Seasat–ERS crossover points are not correlated; the covariance function is then assumed to be a Dirac-delta function. The variance of the residual error is set to $(10 \text{ cm})^2$.

e_{orb} is the residual orbit error after the interpolation of the precise orbit. The orbit error is dominated by frequencies of around 1 cycle per revolution mainly due to error in the gravity field and erroneous initial elements in the orbit. The arcs are very short and the orbit error for each one is nearly a bias; the orbit covariance error can thus be described by a cosine with an exponential damping (Chelton and Schlax, 1993). Because of its large geographical wavelength, the residual orbit error is probably one of the most critical errors. In order to ensure a good constraint on this error, we removed $\delta^{i,j}h(x,y)$ data for which either track i of Seasat or track j of ERS has less than three crossover points on the whole sector. Note that Seasat tracks cross the area from east to west and are thus quite long, while ERS tracks are oriented north–south and are thus quite short. The non-orbital differences of height between ERS ascending paths and descending paths are constant along each track and can be included within the orbit error. The a priori variances for both orbits are thus $(1 \text{ m})^2$.

Note that the unresolved geographically correlated orbit errors (Schrama, 1992) cannot be modeled and corrected for at the present time. To our knowledge, no study of this subject has been done over Antarctica with multiple satellites. This error is inherent in the problem of comparison between two satellites but should mostly be of long wavelength.
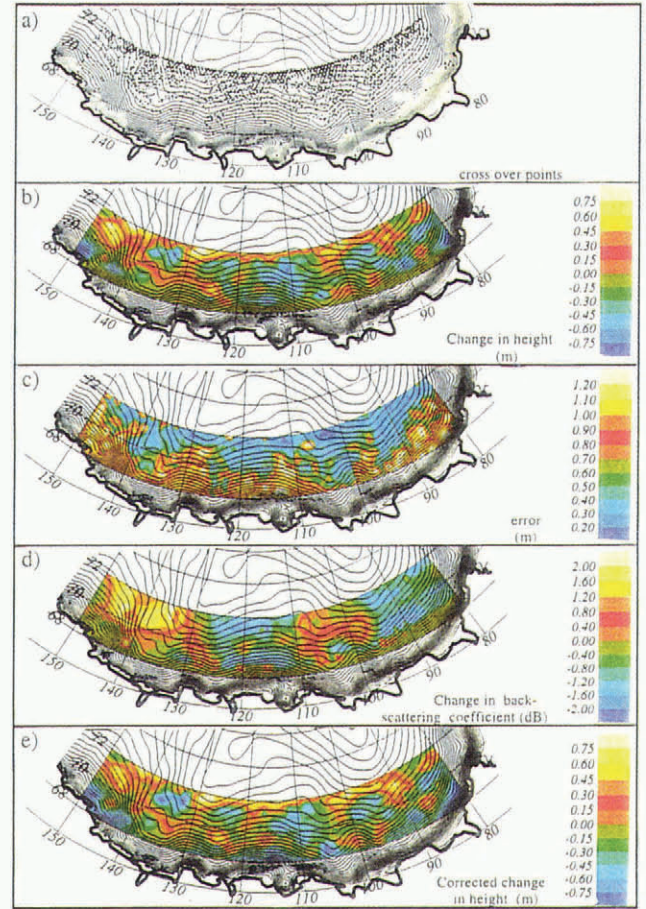

Fig. 1. Sequence of treatment of comparison between Seasat and ERS-1 data north of 72° S in Antarctica. The isoline represents the topography elevation from Brisset and Rémy (1996). (a) Distribution of Seasat–ERS crossover points. (b) Inversion of residual change in height between both missions. (c) Estimated error. (d) Change in backscattering coefficient related to change in snow characteristics. (e) Change in height corrected for change in snow characteristics.

e_{slope} is the slope-induced error. It is due to the shift of the impact point in the upslope direction, and linearly depends on the satellite altitude. Due to an approximately 20 km difference between the altitudes of the two satellites, this error must be corrected for. At each crossover point, we estimate both surface slope and surface curvature from the precise ERS-1 topography (Brisset and Rémy, 1996) and apply a slope correction.

e_{ret} is the difference in retracking error depending on the antenna characteristics. Indeed, Legrésy and Rémy (1997) pointed out that the complex convolution between km-scale topographic features and subsurface signal leads to a non-linear behavior of the waveform in front of subsurface signal intensity that depends on antenna gain characteristics. They showed that even when Seasat and ERS waveforms are retracked with the same algorithm, the resulting height error has a 10 cm rms km scale and a 5 cm bias. Because of its intrinsic complexity, this error cannot be corrected for but can be approximated using an appropriate covariance function.

Finally, e_{snow} is the error due to change in snow-surface characteristics. It is probably the most critical error; in order to control its effect, the correction is performed only after the data inversion process (see section 2.4).

2.3. Mapping through an inverse technique

The mean difference in height (ERS height minus Seasat height) for the 9000 crossover points is +9 cm. Even after careful checking for all sources of bias, this value must be used with caution (see section 3.1). The variance of the difference in height is 1.8 m². The output grid size is set to 35 km in order to smooth noise due to km-scale topography, and to retain a good geographical sampling. The change in height we are seeking is modeled with a Gaussian function with an a priori variance of $(0.5\,\text{m})^2$ and a decorrelation-length scale of 50 km. After inversion of the covariance matrix, the map of residual difference in height is shown in Figure 1b (the averaged value is removed), while the a posteriori error is shown in Figure 1c. North of 70° S, except between 100° and 110° E, the error is quite large mostly because of the inadequate sampling, so the differences should be ignored for these areas. However, from 145° to 85° E and south of 70° S the differences should be significant; indeed the relative amplitude of the signal is around 1 m, which is more than twice the modeled estimate.

2.4. Change in snow-surface characteristics

For the final term of Equation (1), e_{snow}, the error due to change in snow-surface characteristics, is probably the most critical. Legrésy and Rémy (in press) show that a temporal change in surface microroughness yields an artificial change in altimetric height deduced from the waveform, because of the penetration of the radar wave into the snowpack. The induced error in the estimated height depends on the snow-pack characteristics and can be corrected for with the help of the difference between the two backscattering coefficients, if one assumes that the snowpack characteristics have not significantly changed since the time of Seasat. Figure 1d displays the difference between Seasat and ERS back-scattering coefficients: it varies from −2 to 2 dB, and has for the most part a long wavelength signal of zero mean. The more the backscattering coefficient decreases, the more the surface echo is diminished and thus the lower the surface topography becomes. For the studied area, it yields a height correction of < 30 cm rms. Most of the features observed in Figure 1b are still present on the corrected map (Fig. 1e).

Comparison of Figure 1d with the Seasat backscattering-coefficient map (Rémy and others, 1990) suggests a decrease of katabatic wind intensity in the area of strong winds. No such trend is recorded in the meteorological data. The 3 months of Seasat data probably correspond to a period of strong katabatic wind. Note that the difficulty induced by this kind of error is not specific to the comparison between the two missions. It will probably set the limit in the interpretation of long-term surveys of ice-sheet topography, because of the difficulties in separating an actual volume change from an artificial change due to a long-term trend in snow characteristics.

3. DISCUSSION

3.1. Observations

Even if we are at the limit of precision required for proposing a quantitative interpretation, a qualitative interpretation can still be given over a 220 km × 2900 km belt located between 70° and 72° S, and between 150° and 80° E. Change in ice-sheet height can be due to one or several physical processes: accumulation rate enhancement due to climatic warming (Ohmura and others, 1996), stochastic change in accumulation rate (Oerlemans, 1981; Van der Veen, 1993), change in snow transport (Takahashi and others, 1988), change in outlet ice-flow conditions (Alley and Whillians, 1984; Rémy and Minster, 1997) or Holocene warming response (Huybrecht and Oerlemans, 1988).

As already mentioned, we found an average bias between the two datasets of +9 cm. On a technical level, confidence in this value is very low because of the lack of calibration between both heights and backscattering coefficients. In any case, on a geophysical level, a tentative interpretation is also very poor. In fact, the great limitation of such a study is the short duration of the observations, which does not allow us to separate short- and long-term changes in surface elevation. Errors in the short term can be due to the stochastic fluctuations of accumulation rate (Oerlemans, 1981), or induced firn densification that leads to differences between changes in elevation and changes in ice volume (Van der Veen, 1993). We will assume with Oerlemans (1981) that these random fluctuations of accumulation conditions over Antarctica have a large spatial wavelength and thus hide or obscure any other global-scale signal.

The relative rise of inland areas with respect to areas of lower altitude is clearly observed (see Fig. 1e; 105–130° and 90–100° E). These regions exhibit a rise rate of up to 3.5 cm a⁻¹ for an average accumulation rate of 15 cm a⁻¹ (Ohmura and others, 1996), leading to a relative positive imbalance of 25% locally. This value is consistent with the results of Budd and Warner (1996) who compared observed and computed fluxes. Conversely, a substantial decrease of the elevation of about 3 cm a⁻¹ occurs at lower altitude, for instance directly over the Aurora subglacial basin (see 71° S, 110° E) or above the Astrolabe basin (70° S, 138° E). Note that one can have some confidence in the amplitude of the signal between rise and decrease, given the estimated error.

Our inverse method allows the estimation of the a posteriori error. The mapped error suggests that we are at the limit of the altimeter precision, but it should be remembered that the two previously discussed errors cannot be taken into account in the a posteriori estimation: the change in snow characteristics and the geographically correlated orbit error. We must therefore be very guarded in the following discussion and only suggest some hypotheses. At this time, we do not have corroborating in situ observations to support our hypotheses.

3.2. Some hypotheses

The observation of a relative rise of the high-altitude region with respect to the lower-altitude region goes against the idea of a large-scale signal due to a proportional and systematic increase in accumulation rate. However, the only area that has a different behavior, i.e. that exhibits a rise at a low altitude, of the order of 20–25% of the accumulation rate, is in the eastern part between 140° and 150° E and between 70° and 72° S. Indeed global climate models indicate that this area is the most sensitive to change and is subject to a rise of up to 5 cm a⁻¹ in the case of climate warming (Ohmura and others, 1996). On the other hand, field measurements in Wilkes Land suggest recent increases in snow accumulation at GD03 (69° S, 115.5° E) and GD15 (69° S, 130° E) (Morgan and others, 1991) and from D12 to D60 (north of 68°21′ S around 138° E) (Pourchet and others,

1983). Both field measurements are at too low an altitude to be compared with our results, and furthermore no correlation can exist between the trends of a coastal region and a 200 km inland region (Isaksson and others, 1996).

Some areas where elevation decreases seem to coincide with areas of significant depression of the bedrock. Bedrock topography is displayed in Figure 2, where the superimposed arrows represent the along-slope integrated change in height. Negative values corresponding to surface lowering are represented by arrows directed outwards towards the coast; positive values are represented by arrows directed inland.
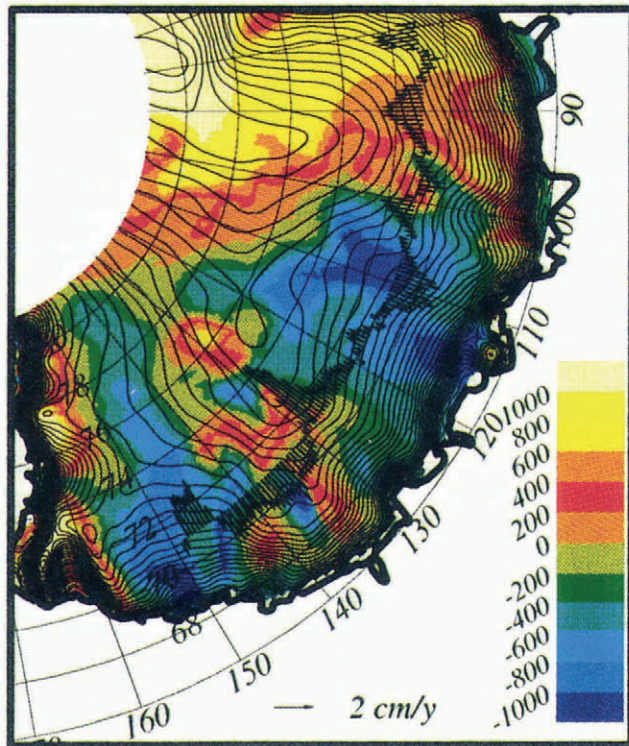

Fig. 2. Bedrock topography map (m) from Drewry (1983). Superimposed arrows represent intensity of along slope averaged in upslope direction. Arrows indicate direction of coast for negative values, and direction of pole for positive values.

One can imagine that the observed lowering signal is due to the Holocene warming that took place at the end of the last glaciation, about 16 000 years ago. But the effect of that warming propagating into the ice is likely to be confined to the upper part of the ice thickness and to have had minimal impact on the deeper basal layers of the ice sheet in this region which is generally above 2500 m (Drewry, 1983; Young and others, 1989).

Part of this signal may be the signature of the sea-level rise induced at the end of the last glaciation. Sea-level rise acts on outlet ice-flow conditions that are diffused upslope (Alley and Whillans, 1984; Rémy and Minster, 1997). This signal, which is exhibited 400 km inland from the coast, could have arisen from a perturbation on the profile at the terminus that happened a few millennia ago (Alley and Whillans, 1984) and whose effect depends of the drainage path. This may have had an influence near the area upslope of Law Dome (68° S, 112° E) and near the area upslope of Dumont d'Urville (67° S, 140° E), that only numerical modelling could verify.

4. CONCLUSION

This paper presents an attempt to compare Seasat and ERS altimetry topography observations of a sector of the Antarctic ice sheet north of 72° S. To improve treatment of the error budget, we use an inverse technique that allows us to take into account statistical knowledge of the errors. This technique, which was developed previously for mapping topography over the ice sheet (Rémy and others, 1989; Brisset and Rémy, 1996), is applied here to correct for orbit error and km-scale errors. The error due to temporal change in snow characteristics (Legrésy and Rémy, in press) is corrected for after the inversion. Data from 9000 crossover points between both missions are inverted, leading to sufficient precision, over a belt between 70° and 72° S and between 150° and 80° E, to allow a qualitative discussion of the results.

Because of the lack of intercalibration between the two missions, we mostly focus on the relative signal and on its spatial signature. The mapped change in height between the missions suggests a rise of the western part of the sector (150–140° E), and of the high-altitude region, corresponding to a positive imbalance of 20% and 25%, respectively. Climate modeling indicates that this western part of the Antarctic is the most sensitive to climate warming (Ohmura and others, 1996), while models do not predict such an enhancement of inland regions. Conversely, observations suggest a decrease of the topography at lower altitude, particularly immediately over bedrock depressions. This could be due to outlet-flow-condition changes associated with sea-level rise at the end of the last glaciation that are transmitted in the upslope direction as suggested by Alley and Whillans (1984).

However, we can only suggest some qualitative explanations of the observations. Both numerical modeling and longer temporal series are required for any quantitative analysis.

ACKNOWLEDGEMENTS

REFERENCES

Alley, R. B. and I. M. Whillans. 1984. Response of the East Antarctica ice sheet to sea-level rise. *J. Geophys. Res.*, **89**(C4), 6487–6493.

Brisset, L. and F. Rémy. 1996. Antarctic topography and kilometre-scale roughness derived from ERS-1 altimetry. *Ann. Glaciol.*, **23**, 374–381.

Budd, W. F. and R. C. Warner. 1996. A computer scheme for rapid calculations of balance-flux distributions. *Ann. Glaciol.*, **23**, 21–27.

Chelton, D. B. and M. G. Schlax. 1993. Spectral characteristics of time-dependent orbit errors in altimeter height measurements. *J. Geophys. Res.*, **98**(C7), 12,579–12,600.

Drewry, D. J. 1983. The surface of the Antarctic ice sheet. *In* Drewry, D.J., *ed. Antarctica: glaciological and geophysical folio.* Cambridge, University of Cambridge. Scott Polar Research Institute, Sheet 2.

Féménias, P., F. Rémy, R. Raizonville and J.F. Minster. 1993. Analysis of satellite-altimeter height measurements above continental ice sheets. *J. Glaciol.*, **39**(133), 591–600.

Huybrechts, P. and J. Oerlemans. 1988. Evolution of the East Antarctic ice sheet: a numerical study of thermo-mechanical response patterns with changing climate. *Ann. Glaciol.*, **11**, 52–59.

Isaksson, E., W. Karlén, N. Gundestrup, P. Mayewski, S. Whitlow and M. Twickler. 1996. A century of accumulation and temperature changes in Dronning Maud Land, Antarctica. *J. Geophys. Res.*, **101** (D3), 7085–7094.

Legrésy, B. and F. Rémy. 1997. Altimetric observations of surface characteristics of the Antarctic ice sheet. *J. Glaciol.*, **43** (144), 265–275; Erratum **43** (145), 596.

Legrésy, B. and F. Rémy. In press. Using the temporal variability of satellite radar altimetric observations to map surface properties of the Antarctic ice sheet. *J. Glaciol.*

Morgan, V. I., I. D. Goodwin, D. M. Etheridge and C. W. Wookey. 1991. Evidence from Antarctic ice cores for recent increases in snow accumulation. *Nature*, **354** (6348), 58–60.

Oerlemans, J. 1981. Effect of irregular fluctuations in Antarctic precipitation on global sea level. *Nature*, **290** (5809), 770–772.

Ohmura, A., M. Wild and L. Bengtsson. 1996. A possible change in mass balance of Greenland and Antarctic ice sheets in the coming century. *J. Climate*, **9** (9), 2124–2135.

Pourchet, M., J. F. Pinglot and C. Lorius. 1983. Some meteorological applications of radioactive fallout measurements in Antarctic snows. *J. Geophys. Res.*, **88** (C10), 6013–6020.

Rémy, F. and J.-F. Minster. 1997. Antarctic ice sheet curvature and its relation with ice flow and boundary conditions. *Geophys. Res. Lett.*, **24** (9), 1039–1042.

Rémy, F., P. Mazzega, S. Houry, C. Brossier and J. F. Minster. 1989. Mapping of the topography of continental ice by inversion of satellite-altimeter data. *J. Glaciol.*, **35** (119), 98–107.

Rémy, F., C. Brossier and J. F. Minster. 1990. Intensity of satellite radar-altimeter return power over continental ice: a potential measurement of katabatic wind intensity. *J. Glaciol.*, **36** (123), 133–142.

Ridley, J. K. and J. L. Bamber. 1995. Antarctic field measurements of radar backscatter from snow and comparison with ERS-1 altimeter data. *J. Electromagn. Waves Appl.*, **9** (3), 355–371.

Schrama, E. J. O. 1992. Some remarks on several definitions of geographically correlated errors: consequences for altimetry. *Manuscr. Geod.*, **17**, 282–294.

Takahashi, S., R. Naruse, M. Nakawo and S. Mae. 1988. A bare ice field in east Queen Maud Land, Antarctica, caused by horizontal divergence of drifting snow. *Ann. Glaciol.*, **11**, 156–160.

Van der Veen, C. J. 1993. Interpretation of short-time ice-sheet elevation changes inferred from satellite altimetry. *Climatic Change*, **23** (4), 383–405.

Young, N. W., I. D. Goodwin, N. W. J. Hazelton and R. J. Thwaites. 1989. Measured velocities and ice flow in Wilkes Land, Antarctica. *Ann. Glaciol.*, **12**, 192–197.

Zwally, H. J., A. C. Brenner, J. A. Major, R. A. Bindschadler and J. G. Marsh. 1989. Growth of Greenland ice sheet: measurement. *Science*, **246** (4937), 1587–1589.